FUNDAMENTALS OF VORTEX-INDUCED VIBRATION

Presentation Notes: This page is a series of questions that introduce the audience to the subject of VIV in a uniform and comprehensive manner. Discussion of these questions and their answers assures that everyone has the same comprehensive understanding of what VIV is and why and when it occurs.

Questions

- What is VIV?

- What are the details of a steady approach flow past a stationary cylinder?

  - o To understand VIV, you must first understand the physics of a steady approach flow past a nonvibrating circular cylinder.

- How and why does VIV occur?

- What kind of body shapes experience VIV?

- What kinds of VIV are there?

  - o Self-excited oscillations - this type of VIV is what occurs naturally, i.e., when the vortex-shedding frequency and the natural frequency are approximately the same. (This is the real VIV – this is vortex-induced vibration)
  - o Forced oscillations – occurs at velocities and amplitudes which are preset and can be controlled independently of fluid velocity. (This is not the real VIV – this is vibration-induced vortices).

- How do you eliminate VIV?
  - o This is the ultimate question! It may be best to design around VIV. In other words, let's learn how to predict VIV and then avoid the situations that will produce VIV. The circular cylinder will always be the preferred shape and the fluctuating lift will always be there, VIV or no VIV. Since we can't avoid the shedding of vortices, let's try to learn to avoid the situations that produce VIV.

NOMENCLATURE

f_{vac} **–** the natural frequency of a system as found in a vacuum.

f_{ex} – the frequency of oscillation of a vibrating body (either forced or Self-excited) regardless of whether lock-in is present.

f_{St} – the vortex shedding frequency (Strouhal frequency) of a body at Rest.

f_{vs} – the vortex shedding frequency of a body in motion (forced or self excited). In the lock-in range, f_{vs} becomes increasingly smaller than f_{St} until lock-out.

Re – the Reynolds number (= Ud/v), the ratio of inertia forces to viscous forces.

St – the Strouhal number (=$f_{St}d/U$), the dimensionless vortex Shedding frequency.

KC – Keulegan-Carpenter number (=$U_{max}T/d = U_{max}/f_{ex}d$)

V_r – the reduced velocity (=$U/f_{ex}d$), the approach velocity normalized The the excitation frequency and the diameter.

StV_r - the product of the Strouhal number and the reduced velocity (=$(f_{St}d/U)(U/f_{ex}d) = f_{St}/f_{ex}$)

$1/(StV_r)$ – equals f_{ex}/f_{St}

f_{air} – the natural frequency of a system in air.

f_{wtr} – the natural frequency of a system in water.

ζ – material damping (not fluid damping).

m^* - reduced mass, $= ((m_b/\ell)/\, \rho_f\, \pi d^2/4)$ or $m^* = \rho_m/\rho_b$ with $\rho_m = (m_b/\ell)/(\pi d^2/4)$.

VIV body – a geometric shape, not necessarily a cylinder or even a circular cylinder, which will produce VIV.

$m^*\zeta$ – the mass-damping term.

A/d – the amplitude to diameter ratio.

C_D – Drag Coefficient, $C_D = D/\rho_f\, A_p\, U^2/2$

C_L – Lift Coefficient, $C_L = L/\rho_f\, A_p\, U^2/2$

C_M – Inertia Coefficient, $C_M = F_I/(\rho_f Vol\; dU/dt)$

Added Mass – the increase in effective mass that occurs when the acceleration of a body is nonzero. This is also called the hydrodynamic mass. The inference is that the effective mass is the sum of the mass of the body and the added mass. The added mass doesn't influence the situation until there is acceleration.
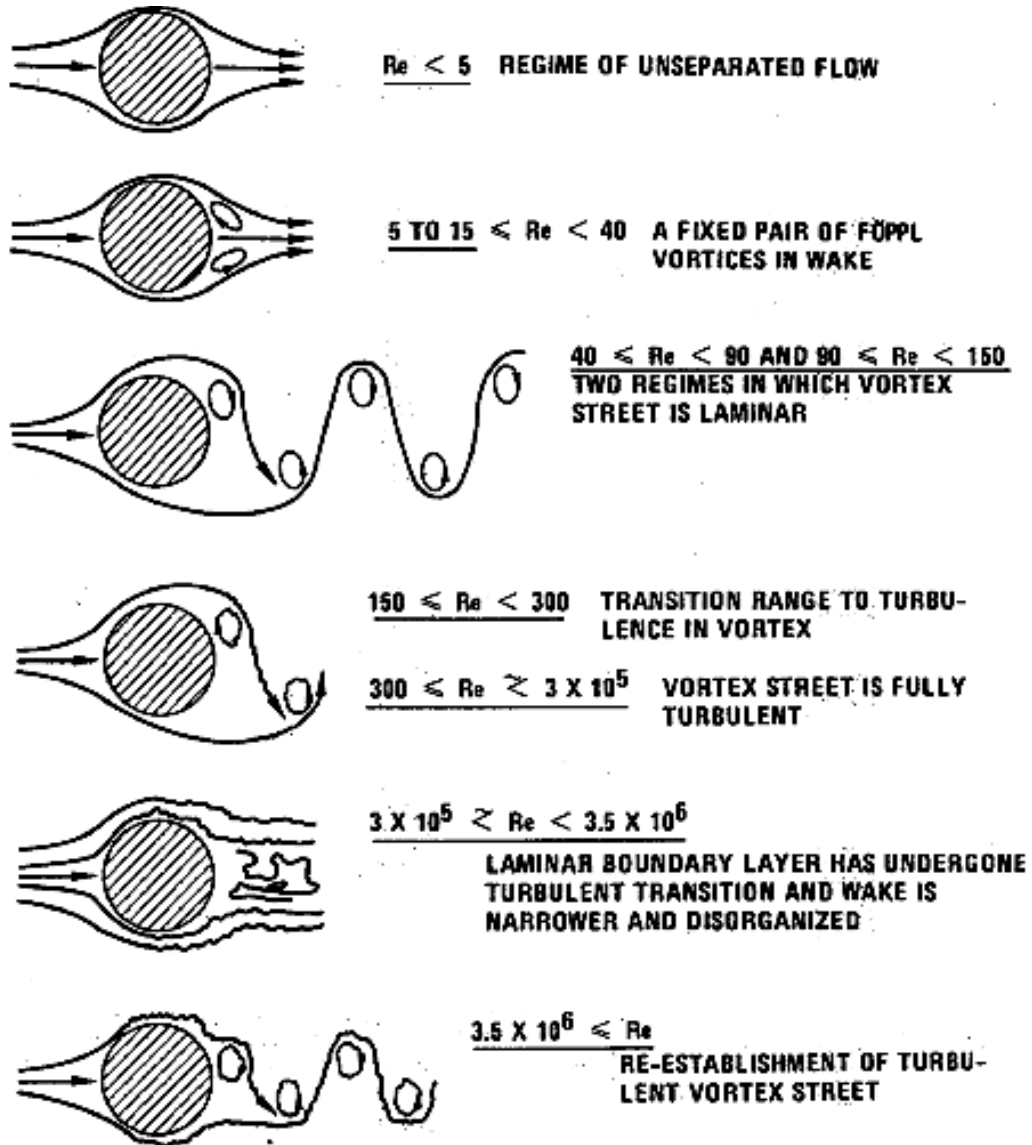
Presentation Notes: Figure 1 is a plot of the drag coefficient (C_d) versus Reynolds number (Re) for a steady approach flow past a circular cylinder. Figure 2 is a schematic diagram which shows the various regimes of the flow past a circular cylinder. These two figures are discussed simultaneously so that the meaning of the various aspects of the drag-coefficient/Reynolds-number plot can be fully understood.

Figure 1: Flow around a circular cylinder
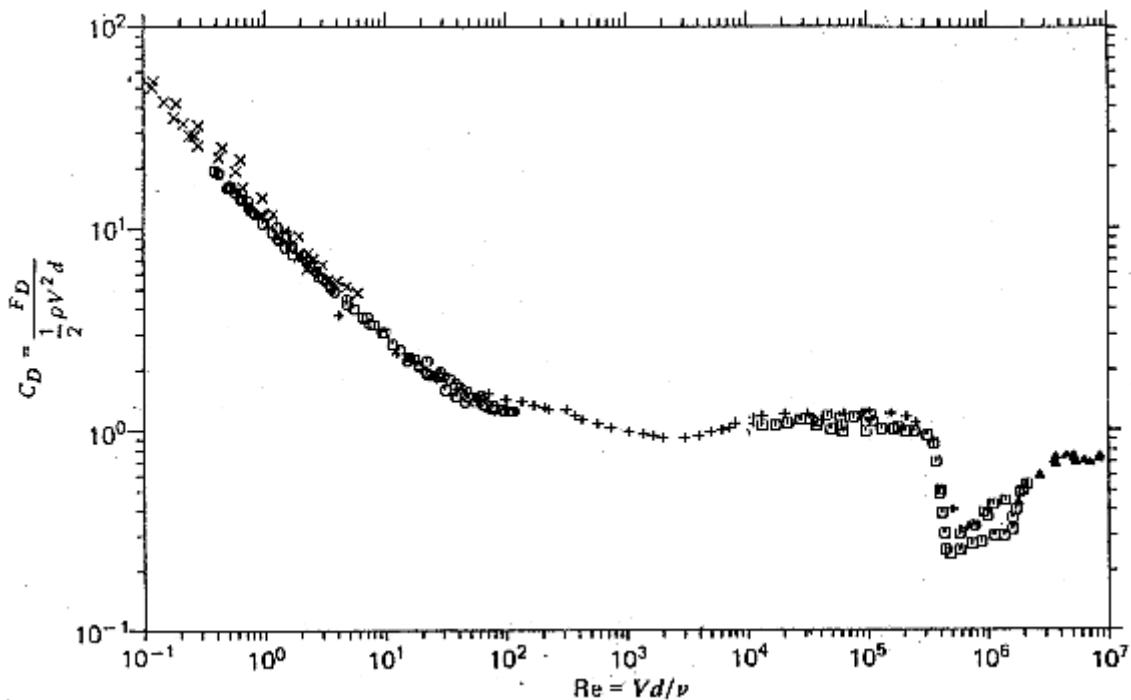
Drag and Curve for a cylinder. Data is from Delany and Sorenson (1953), Finn (1953), Roshko (1961), Tritton (1959) and Wieselsberger (1921)

Figure 2: Regimes of fluid flow across smooth circular cylinders (Lienhard, 1966)

Re < 5 REGIME OF UNSEPARATED FLOW

5 TO 15 ≤ Re < 40 A FIXED PAIR OF FÖPPL VORTICES IN WAKE

40 ≤ Re < 90 AND 90 ≤ Re < 150 TWO REGIMES IN WHICH VORTEX STREET IS LAMINAR

150 ≤ Re < 300 TRANSITION RANGE TO TURBU-LENCE IN VORTEX

$300 \leq Re \gtrsim 3 \times 10^5$ VORTEX STREET IS FULLY TURBULENT

$3 \times 10^5 \gtrsim Re < 3.5 \times 10^6$

LAMINAR BOUNDARY LAYER HAS UNDERGONE TURBULENT TRANSITION AND WAKE IS NARROWER AND DISORGANIZED

$3.5 \times 10^6 \leq Re$

RE-ESTABLISHMENT OF TURBU-LENT VORTEX STREET

Presentation Notes: This figure is a plot showing the Strouhal number (St, St=Df$_{vs}$/U) versus the Reynolds number (Re, Re=UD/ν). The variation of St with Re is discussed so that the audience has an understanding of what flow features influence St, i.e., the vortex shedding frequency, and why they do so.

Figure 3: Strouhal number − Reynolds number relationship for circular cylinders
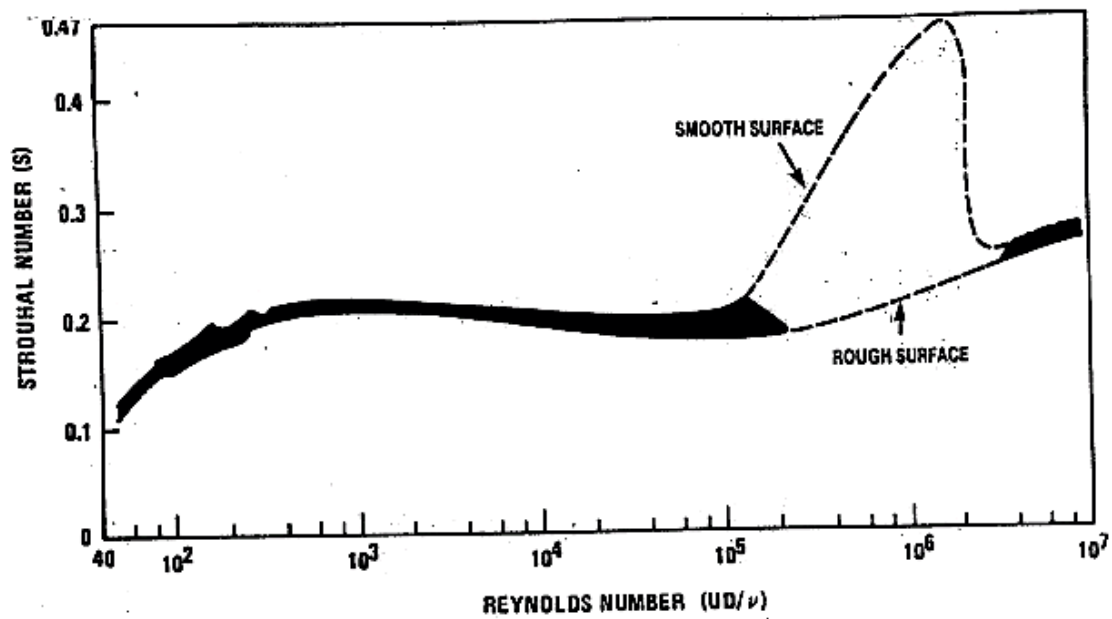
(Lienhard, 1966; Achenbach and Heinecke, 1981). S $\cong$ 0.21 (1-21/Re) for 40<Re<200 (Roshko, 1955).

Presentation notes: This is a plot which shows how the rms lift coefficient (C_L) is influenced by the length-to-diameter ratio (L/D) of the cylinder at different values of the Reynolds number (Re). From this plot it is clear that the cylinder must have an L/D value of at least 6.7 for end effects to lose their influence on the flow field and, hence, the drag acting on the cylinder.

Figure 4: The fluctuating lift coefficient vs. Reynolds number for different aspect ratios.
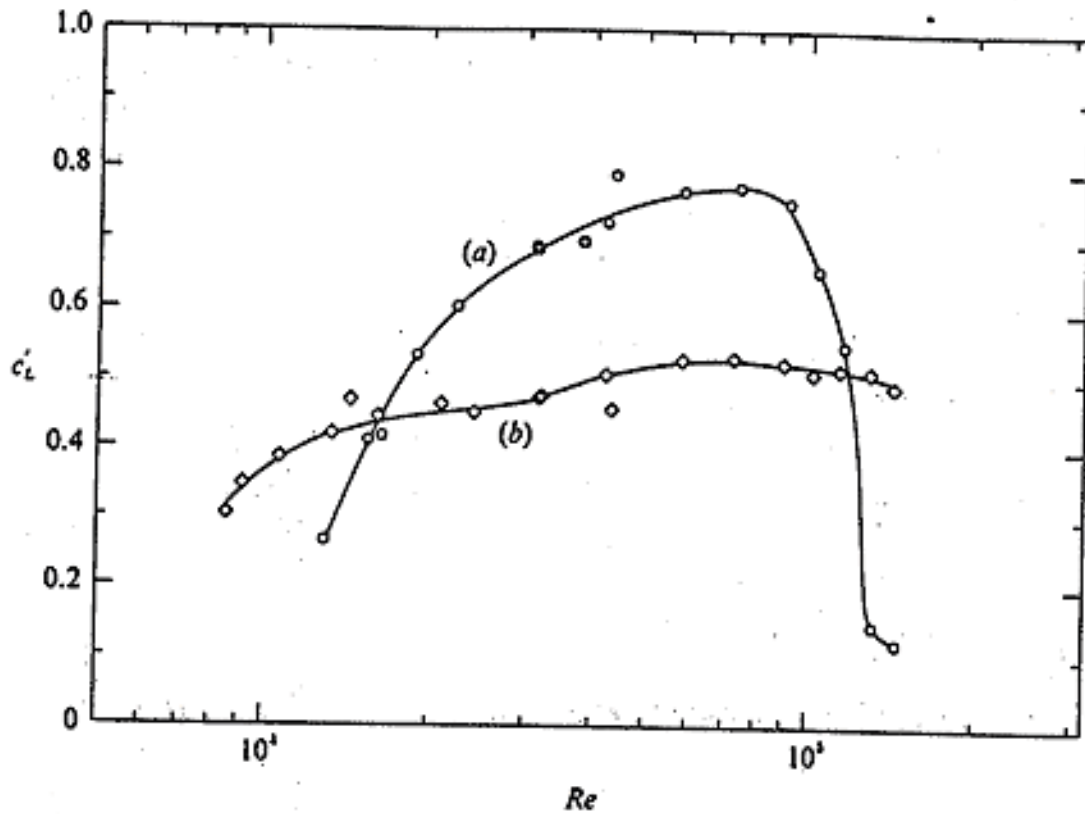
(a)   L/D =1, (b) L/D = 6.7
From Szepessy & Bearman (1992)

Presentation Notes: This is a plot which shows the vortex structure and the circumferential pressure distribution (actually the pressure coefficient) over about one-third of a vortex-shedding cycle. This figure illustrates quite clearly how and why the vortex structures change with time. Also shown is the circumferential pressure coefficient variation. From these plots, it becomes quite clear that the lift coefficient fluctuates about a zero mean value and the instantaneous drag coefficient fluctuates about the mean value of the drag coefficient, although at a much smaller oscillatory amplitude than the lift coefficient.

Figure 5: A sequence of simultaneous surface pressure fields and wake forms at Re=112000 for approximately 1/3 of one cycle of vortex shedding. (Drescher, 1956)
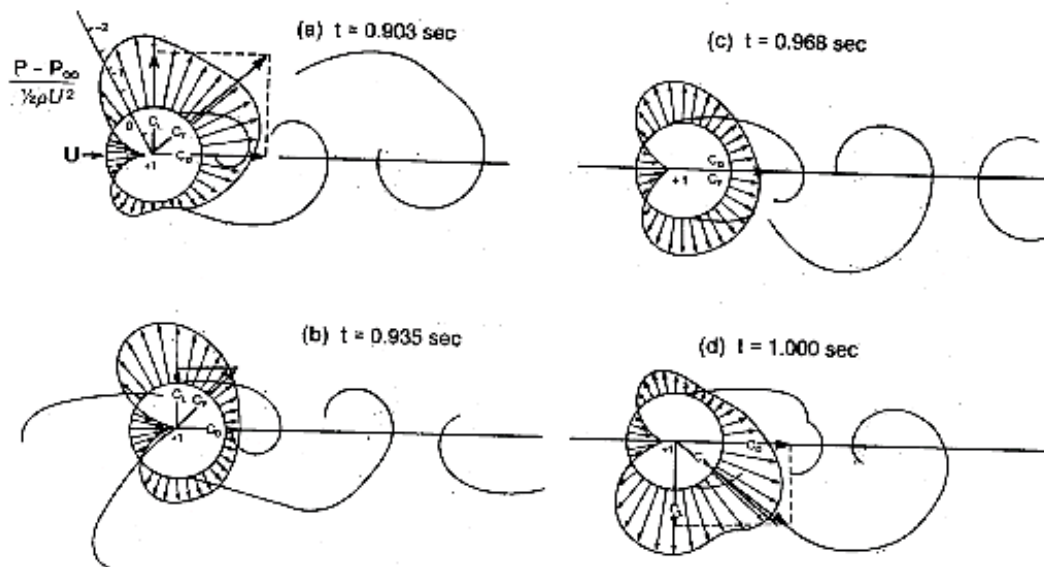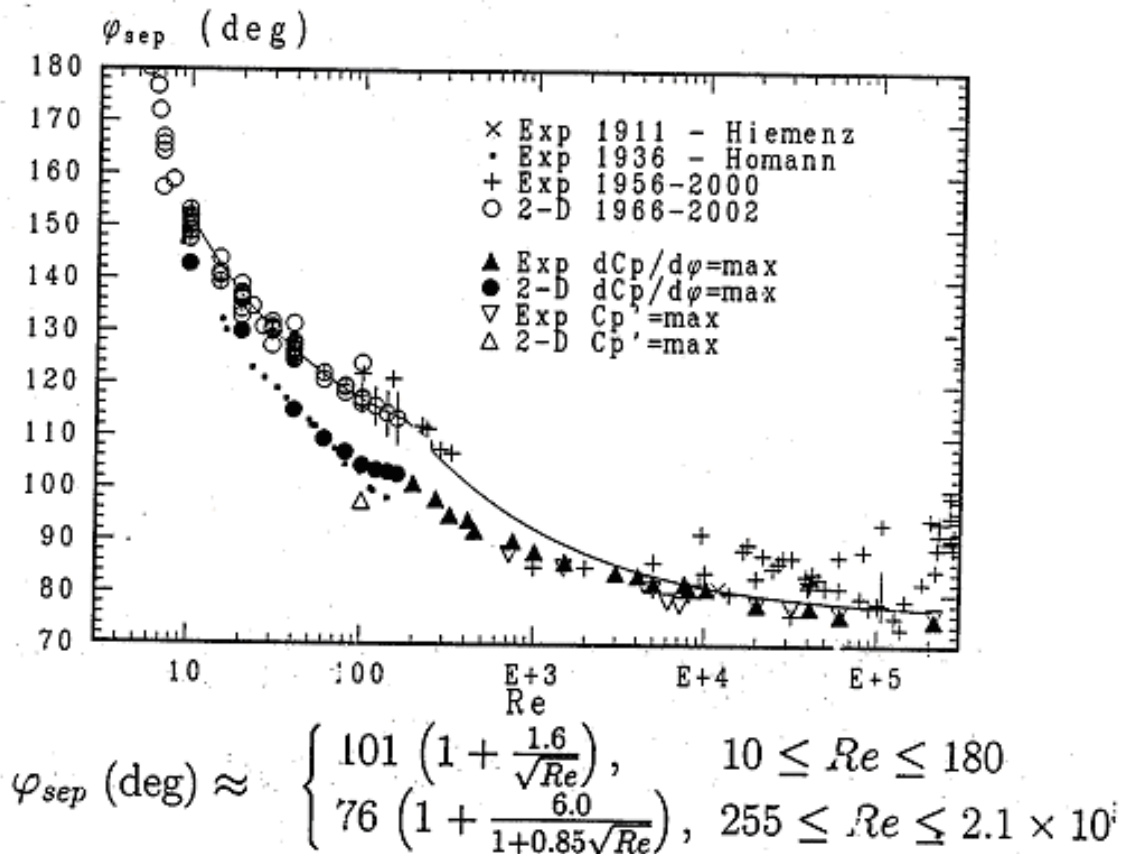
Presentation Notes: This is a plot of the time-dependent pressure coefficient (C_p) versus the angular position (Θ). The time-dependent nature of C_p (mostly) in the cylinder wake ($50°<\theta<310°$) shows how the wake pressure varies with time which explains how and why the time-dependent lift force occurs. The usual time-mean pressure coefficient has an average lift-coefficient of zero.

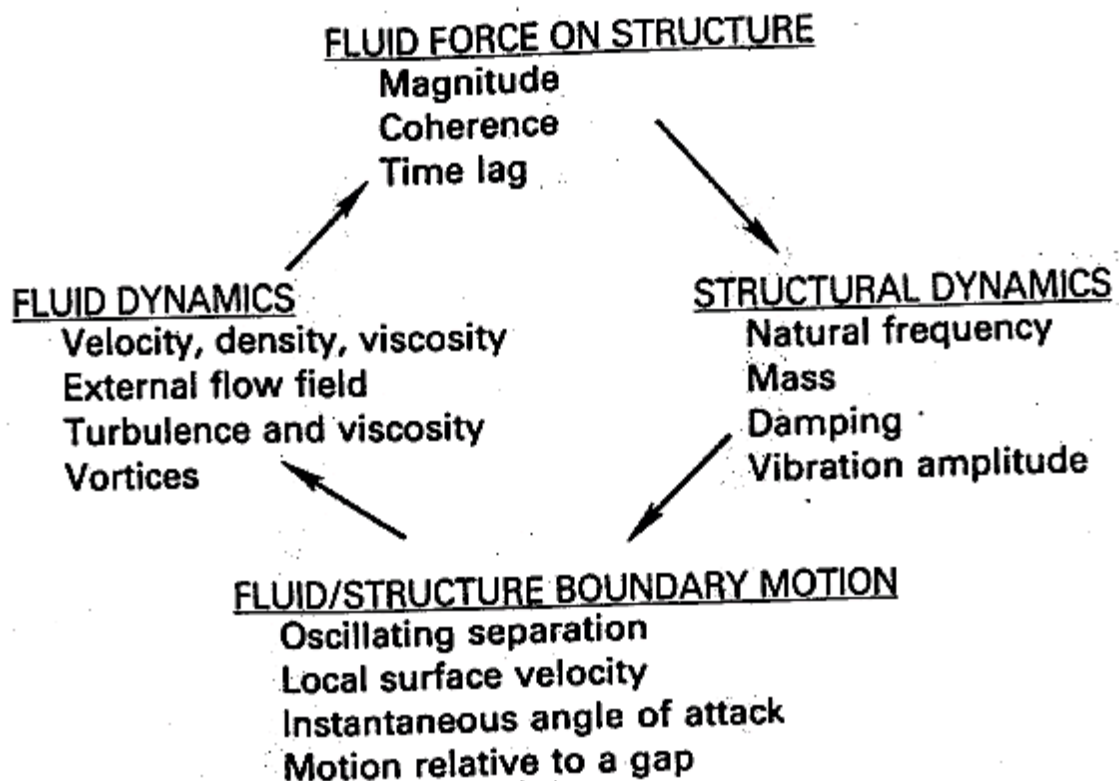**Figure 6: Time-dependent pressure coefficient (C_p) vs. angular position (θ)**
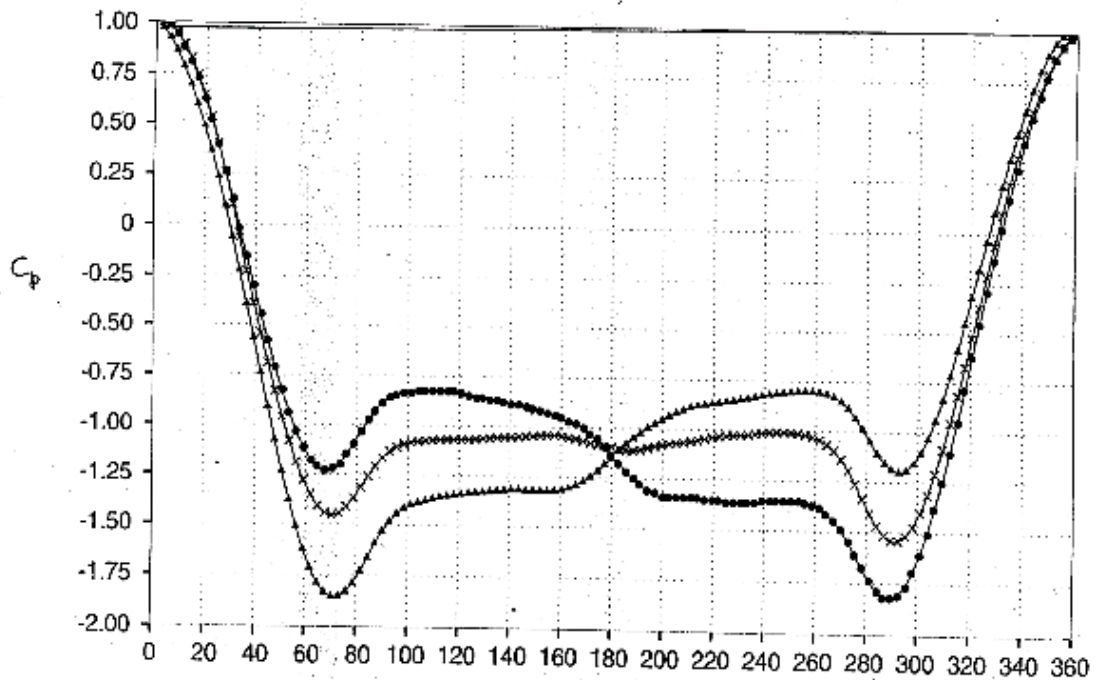
Presentation Notes: This is a plot which shows how the location of the separation angle (θ_{sep}) depends on the Reynolds number (Re). Note that θ_{sep} is decreasing toward a value of about 80° as Re approaches a value of about 2 x 10^5 at which point θ_{sep} begins to increase. The reason for the increase is that the boundary layer on the cylinder experiences a transition to turbulence at this Reynolds number and the separation point increases from about 80° to about 110° to 120° when the boundary layer becomes turbulent

Figure 7: Separation Angle

$$\varphi_{sep} \text{ (deg)} \approx \begin{cases} 101\left(1+\frac{1.6}{\sqrt{Re}}\right), & 10 \leq Re \leq 180 \\ 76\left(1+\frac{6.0}{1+0.85\sqrt{Re}}\right), & 255 \leq Re \leq 2.1 \times 10^5 \end{cases}$$

Presentation Notes: This is a schematic showing the fluid-structure interaction relationship when VIV occurs. When the cylinder isn't vibrating, there is still a time-dependent force acting on the cylinder. This is represented in the top and left segments of the figure. When the cylinder vibrates, all four segments of the schematic are involved in the relationship describing the cylinder response.

Figure 8: Feedback between fluid and structure.

FLUID FORCE ON STRUCTURE
Magnitude
Coherence
Time lag

FLUID DYNAMICS
Velocity, density, viscosity
External flow field
Turbulence and viscosity
Vortices

STRUCTURAL DYNAMICS
Natural frequency
Mass
Damping
Vibration amplitude

FLUID/STRUCTURE BOUNDARY MOTION
Oscillating separation
Local surface velocity
Instantaneous angle of attack
Motion relative to a gap

Presentation Notes: Figure 9 is a plot showing the map of the different wake structures that occur in a <u>forced</u> oscillation, i.e., one occurring when the cylinder is forced by an external forcing function to oscillate at a prescribed amplitude and frequency. The wake structure that would be present in a forced oscillation depends on the amplitude-to-diameter ratio (A/D) and the ratio of the excitation period to vortex-shedding period (T_e/T_v). It is not expected that these same patterns will occur when the cylinder motion is self-excited
(at a sufficiently high Reynolds number, i.e., Re$\geq\sim$5000) which infers the oscillation is neither at constant amplitude nor constant period. Figure 10 shows a more detailed representation of each of the vortex-wake patterns.

Figure 9: Map of vortex synchronization patterns near the fundamental lock-in region.
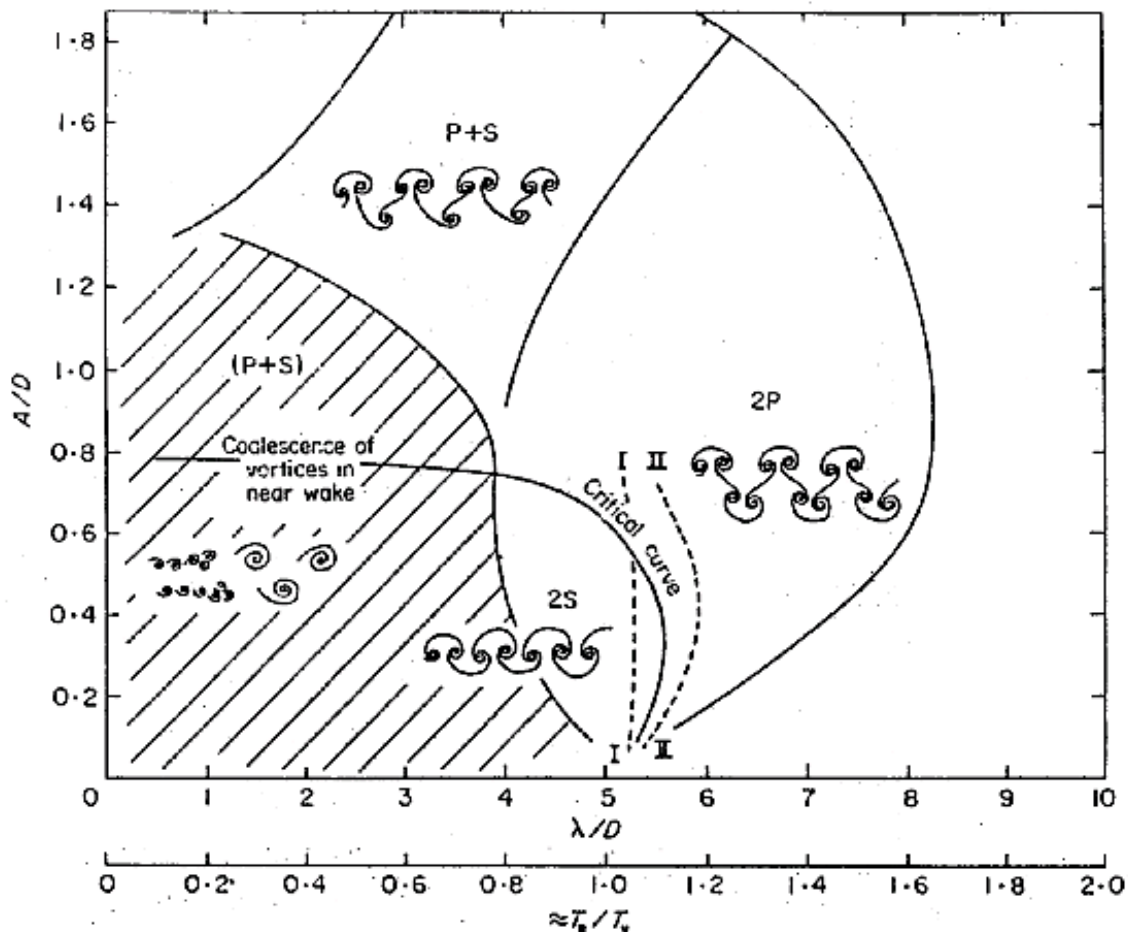
The critical curve marks the transition from one mode of vortex formation to another. I, II are the curves where the forces on the body show a sharp "jump"; from Bishop and Hassan {3}. I is for wavelength decreasing and II is for wavelength increasing.

Figure 10: Sketches of the vortex shedding patterns found in figure 9 (previous)
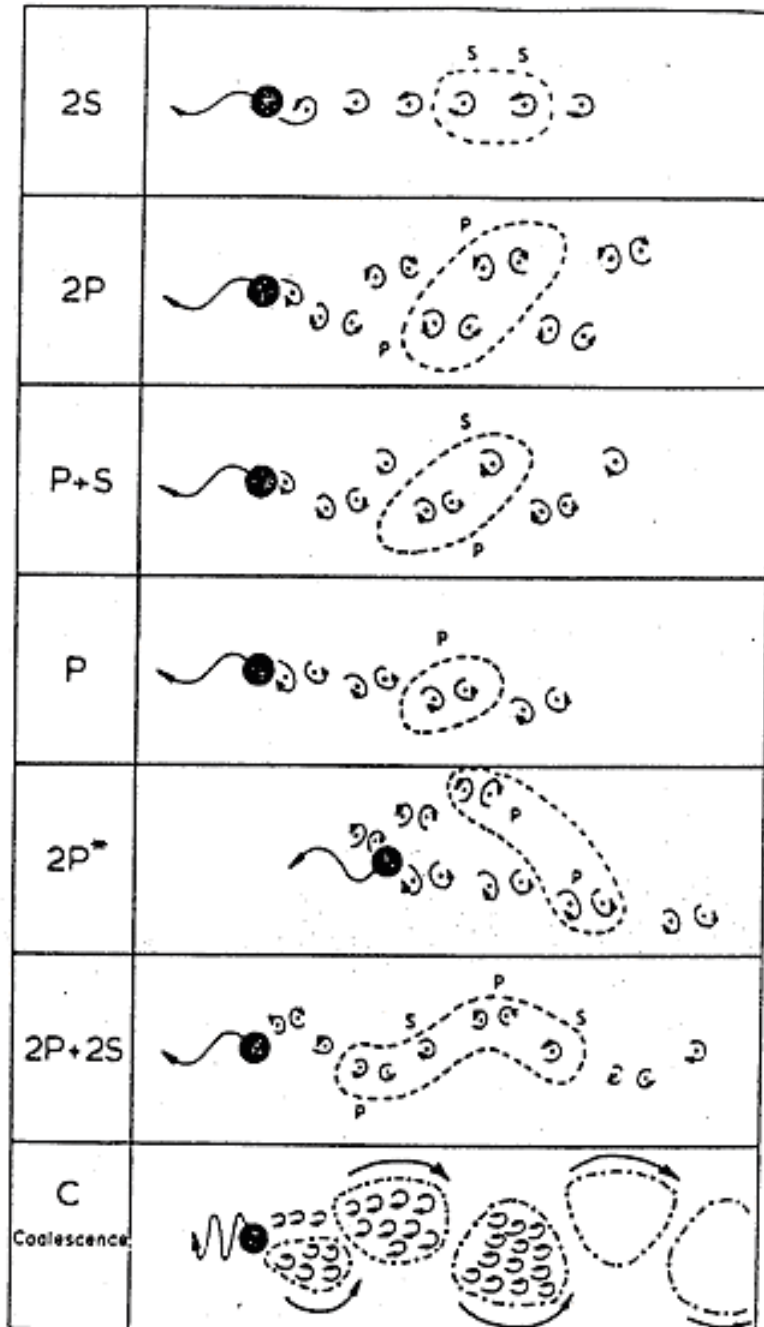
"P" means a vortex pair and "S" means a single vortex, and each pattern is defined by the number of pairs and single vortices formed per cycle; ------ encircles the vortices shed in one complete cycle.

Presentation notes: This figure is the classical self-excited oscillation plot showing the lock-on nature of the cylinder oscillation in self-excited conditions. The two features of the plot show the reduced velocity ($Vr=U/f_{air}D$) plotted against both the amplitude-to-diameter ration (A/D) and the ratio of vortex-shedding frequency to natural frequency (fs/f). The plot shows the sudden increase in oscillation amplitude at $Vr \cong 5$. This lock-on continues to $Vr \cong 7$.

Figure 11: Vortex-induced vibration of spring-supported, damped circular cylinder.
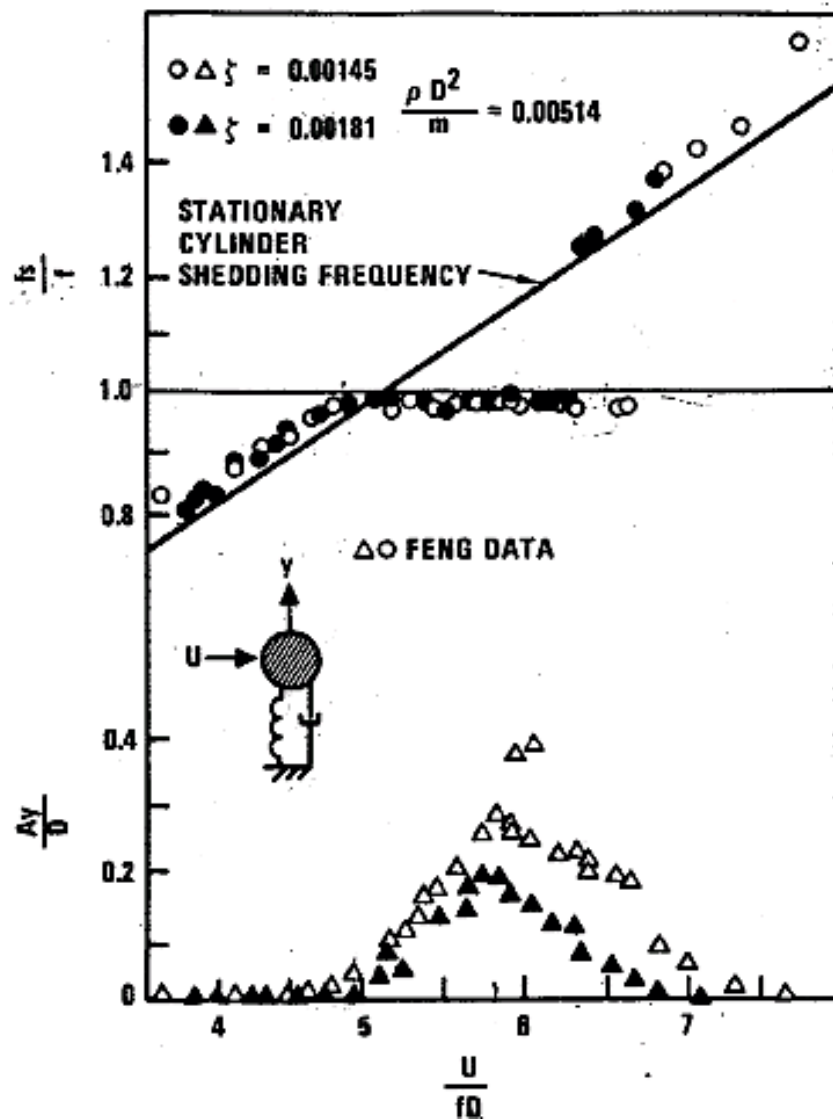
f is the natural frequency of the cylinder (Feng, 1968)

Presentation Notes: This figure shows the lock-on phenomenon also. It has an additional feature for self-excited oscillation. The phase angle, which is the angle by which the force leads the displacement, is also shown. The phase angle is noted to have values that range from about -10° to about 100°. The A/D plot shows what is known as the upper and lower branches of oscillations which are due to a hysteresis effect when the reduced velocity is either increased or decreased.

Figure 12: Response and wakes characteristics of a spring-mounted cylinder freely oscillating in air.
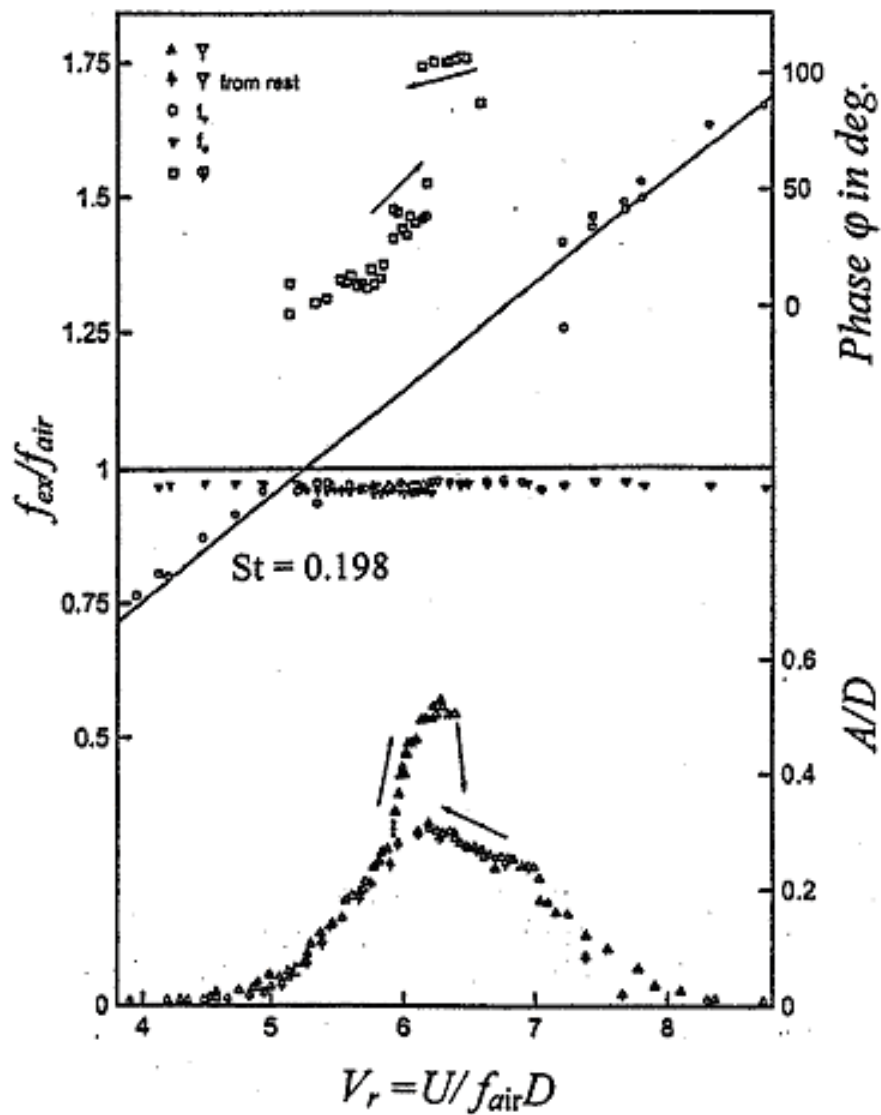
$m* = 248$, $\zeta = 0.00103$, $m*\zeta = 0.255$, and Re (varying with $V_r = U/f_{air}D$) from 10^4 to 5×10^4 (Feng, 1968)

Presentation Notes: This plot also shows the lock-on behavior. However, this plot contrasts the forced oscillation results of Khalak & Williamson with the self-excited results of Feng. The difference between the two sets of results is quite distinct.

Figure 13: Comparison of Feng's vs. Khalak & Williamson data

$$V_r = U/f_{wtr}D$$

$$V_r = U/f_{air}D$$
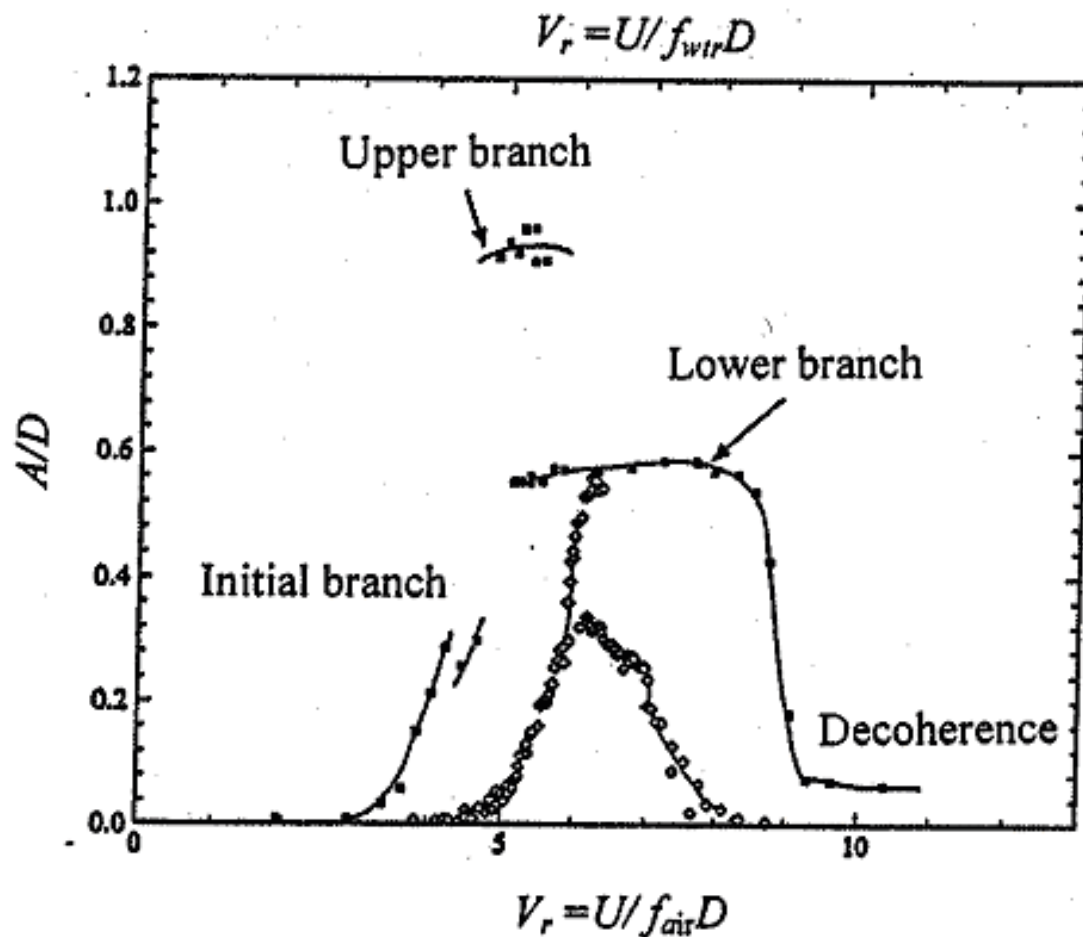
A comparison of Feng's maximum A/D vs. fex/fair data with those obtained by Khalak and Williamson (1999) in water with a single-degree-of-freedom flexible cylinder (m*=10.1, ζ =0.0013, m*ζ=0.013). Feng's data has only two branches (initial and lower). The Khalak and Williamson data (A/D vs. U/fwtrD) have three branches (initial, upper, and lower), much larger peak amplitude, and broader synchronization range.

Figure 14: Variation of the shedding frequency with the driving frequency of a single cylinder in uniform flow.
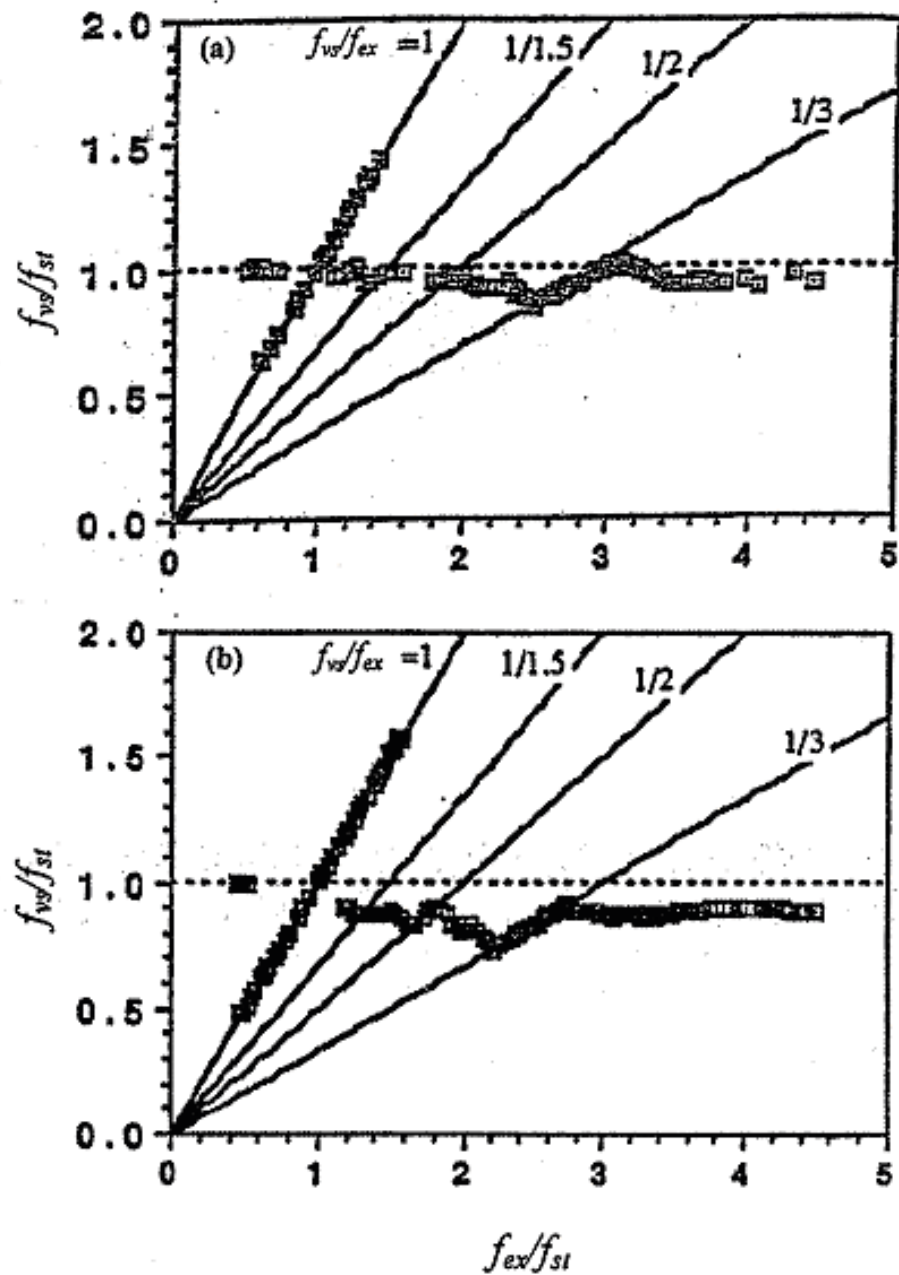
(a)   A/D=0.05, Re=1500; and (b) A/D=0.235, Re=1500
(Cheng and Moretti, 1991)

18

Presentation Notes: This plot shows essentially the comparison of the vortex shedding frequency f_{vs} vs. the excitation frequency f_{ex} in a forced oscillation case. The lock-on behavior is shown more prominently for the case of $f_{vs}/f_{ex}=1$.

Figure 15: The normalized wake frequencies as a function of the normalized oscillation frequency, vortex shedding frequency, and remaining wake frequencies for A/D=0.22 and Re=1500. (Krishnamoorthy, Price, and Paidoussis, 2001).
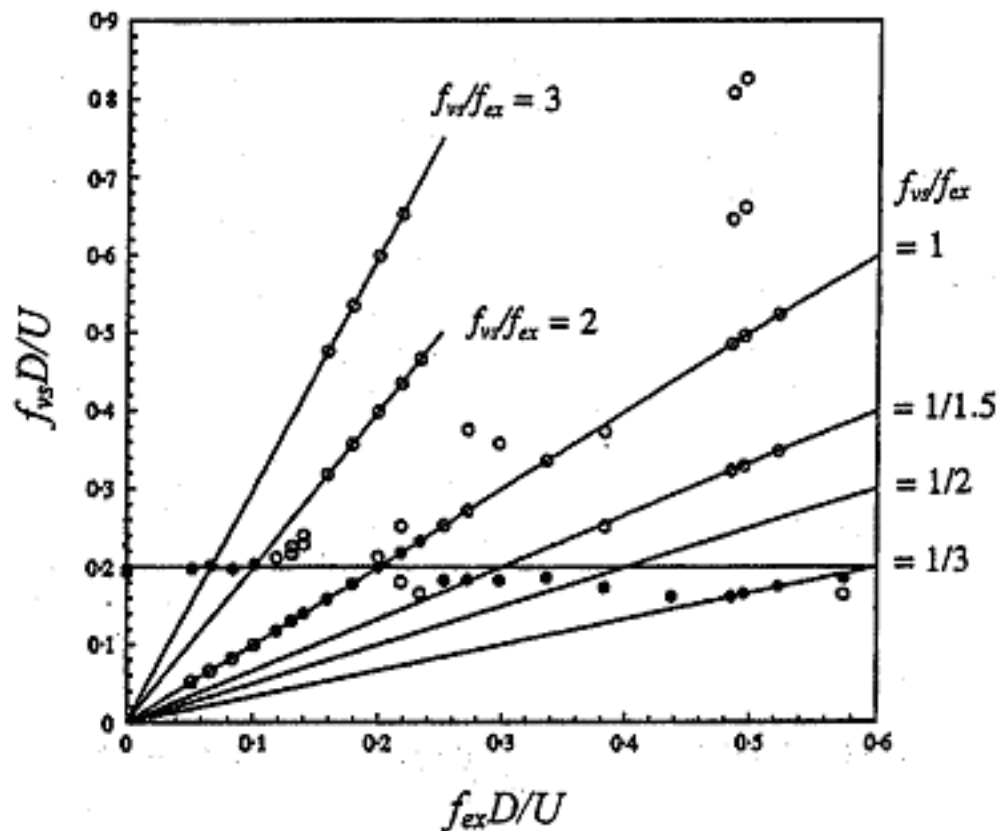
Presentation Notes: This series of plots shows the Griffin response parameter S_G versus A/D with the shape factor λ included for several different representations. The term λ takes on different values for different cylinder shapes.

Figure 16: Experimental measurements of a modally normalized maximum amplitude vs. the response parameter S_G and the proposed curve-fit (Eq. 4)
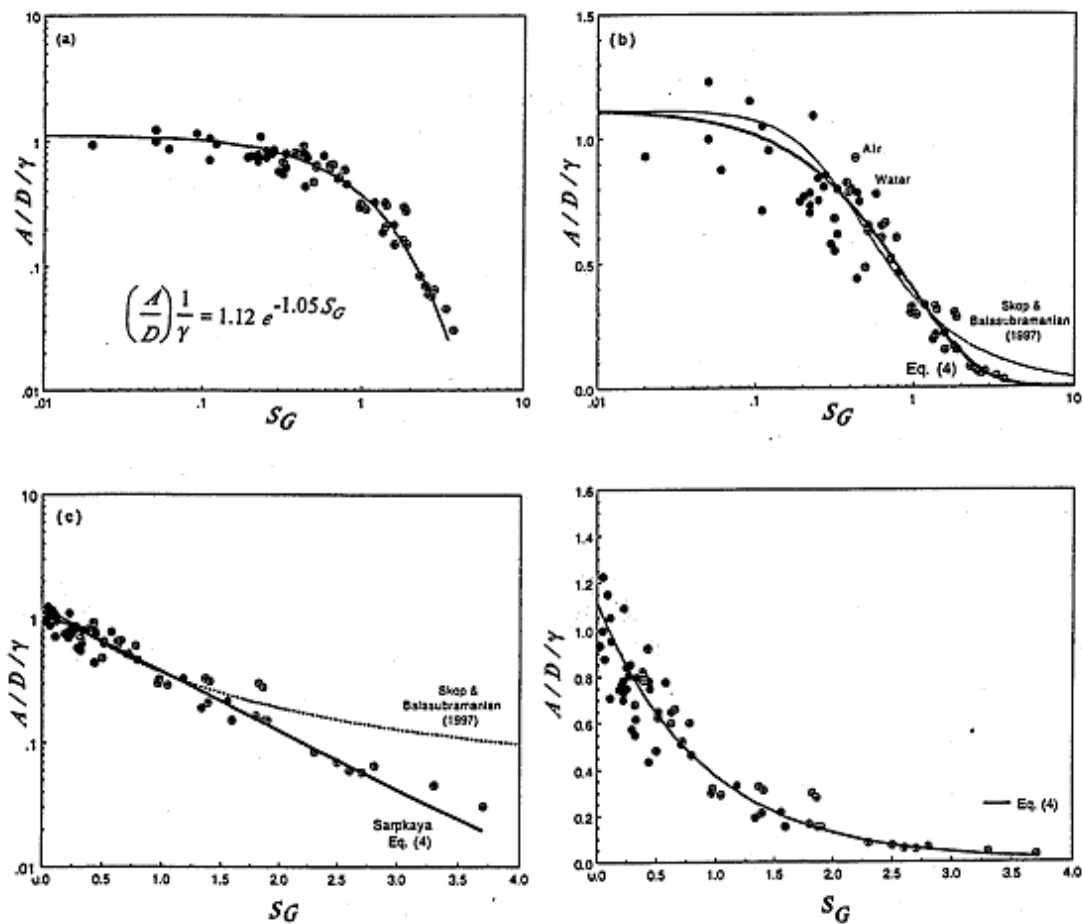
The data is tabulated in Skop and Balasubramanian (1997). The above figures show: (a) a Log-Log plot, (b) a linear-Log plot, (c) a Log-linear plot, and (d) a linear-linear plot. In each case, Eq. (4) represents the data reasonably well and makes an unrigorous but plausible suggestion that Ln (A/D/y) may be a linear function of S_G.

Presentation Notes: These two plots show a comparison of the results for forced and free vibrations, both for the same reduced velocity. The phase angle difference between the two cases is quite distinct.

Figure 17: Forced and free vibrations
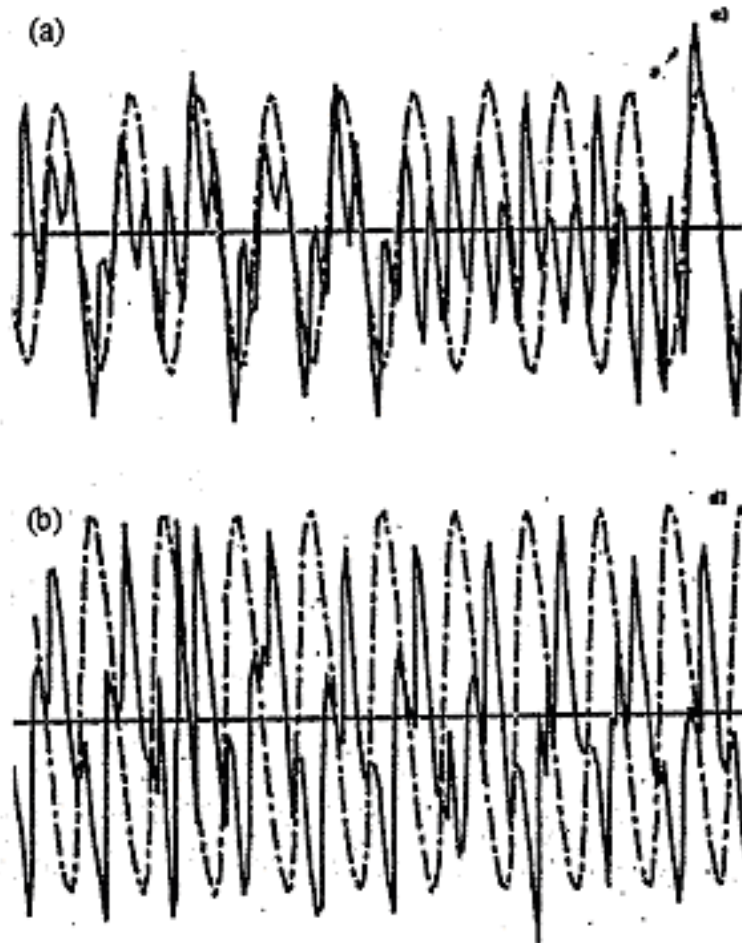
Sample data show that perfect synchronization is not "perfect" and 10% variation in peak amplitudes of force (in both forced and self-excited oscillations) is quite common; (a) self-excited, in-line spring-supported, V_r=5.93; (b) forced, in-line spring-supported, V_r=5.93 (from Moe and Wu, 1990).

Presentation Notes: This plot shows the variation of the added mass coefficient (C_a), the drag coefficient (C_d) and the phase angle vs. f_{ex}/f_{st}. Note the very sharp decrease in phase angle at $f_{ex}/f_{st} \cong 0.85$ and the increase in C_a at the same frequency ratio value.

Figure 18: Inertia and drag coefficients (or the in-phase and out-of-phase components of the lift force) and the phase angle as a function of f_{ex}/f_{St}
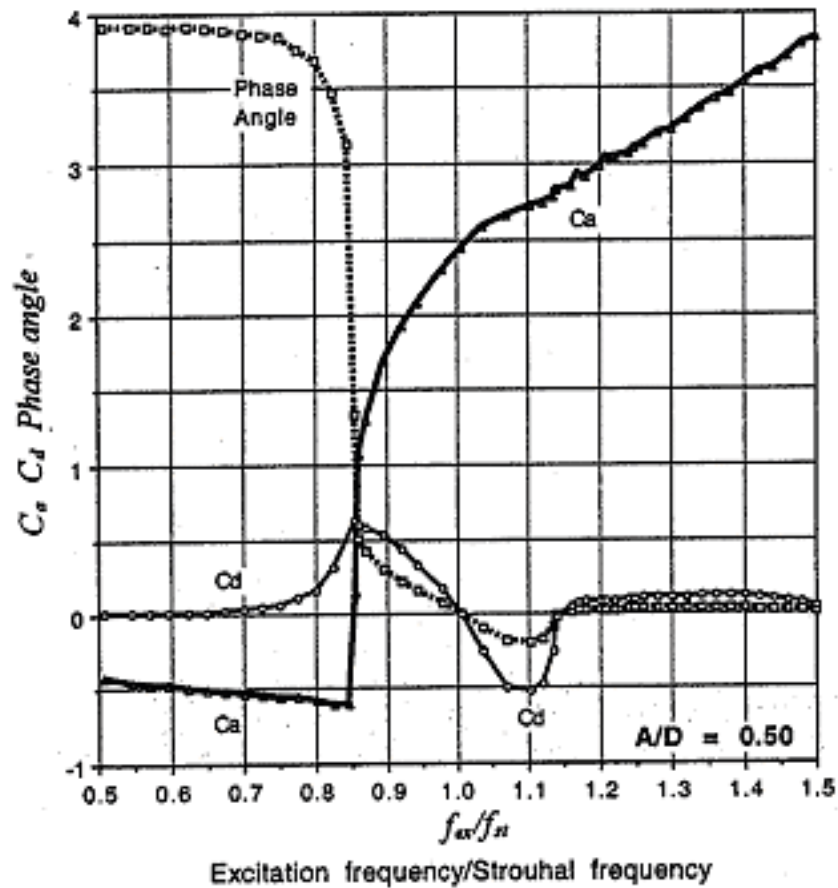
(A/D=0.50, Re=42,500, L/D=7, smooth cylinder) (from author's experiments). Perfect synchronization is seen to occur at $f_{ex}/f_{St} \cong 0.85$, accompanied by abrupt changes in phase and force-transfer coefficients.

Presentation Notes: This is essentially the same plot as in Figure 18, except that the abscissa is the reduced velocity Vr(=$U/f_{ex}D$). The effect here is essentially the opposite of that shown in Figure 19. The phase angle shows a very sharp increase at Vr $\cong$ 5.8 with increasing Vr while C_a shows a sharp decrease at Vr $\cong$ 5.8.

Figure 19: Inertia and drag coefficients (or the in-phase and out-of-phase components of the lift force) and the phase angle as a Function of $V_r=U/f_{ex}D$
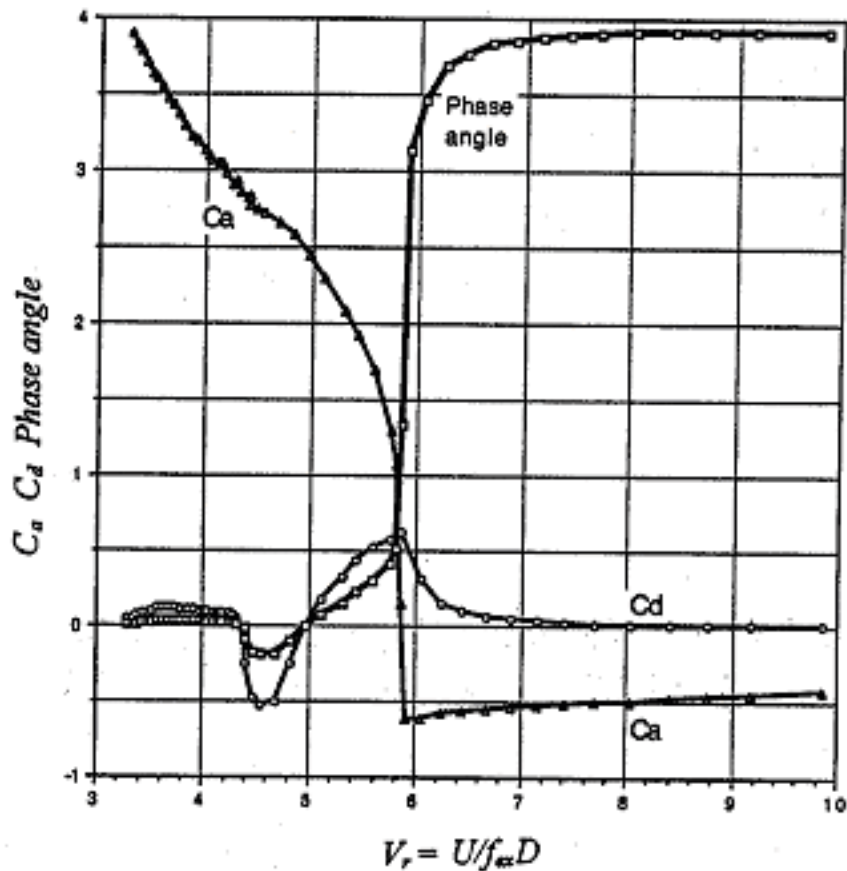
(A/D=0.50, Re=42,500, L/D=7, smooth cylinder)(from author's experiments). Perfect synchronization is seen to occur at V_r=5.80-5.85, accompanied by abrupt changes in phase and force-transfer coefficients (same as figure 18 except that the horizontal axis is changed to V_r).

Figure 20: Instantaneous streamlines (left) and vorticity contours (right) for various f_{ex}/f_{St}.

$f_e/f_o = 0.9$

$f_e/f_o = 0.95$

$f_e/f_o = 1.0$

$f_e/f_o = 1.05$
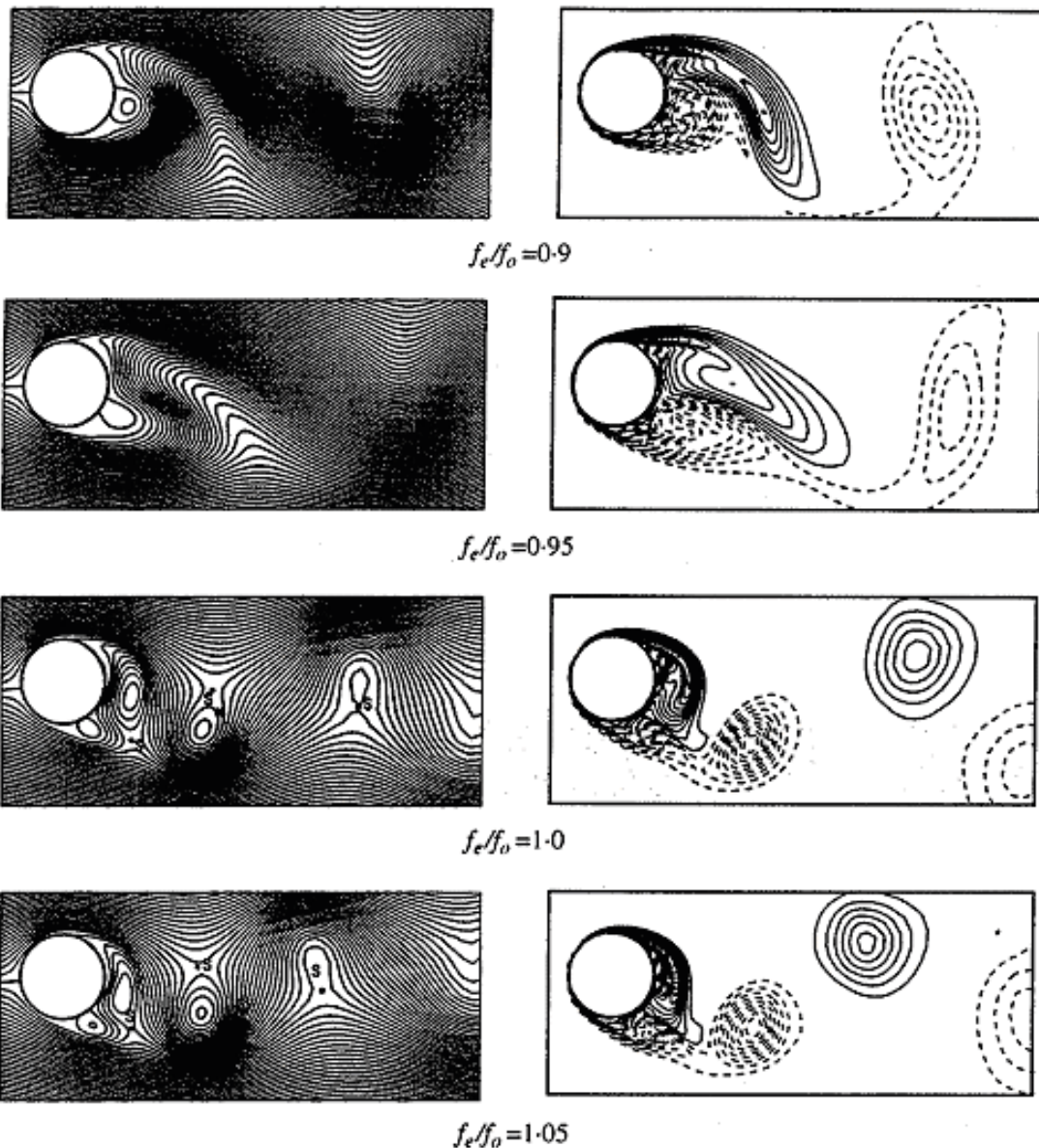
A/D=0.4, Re=1000. In all cases, the location of the cylinder is at its extreme upper position. At $f_{ex}/f_{St}=0.95$, a new vortex is being shed from the upper surface. However, at $f_{ex}/f_{St}=1.0$, the shedding of a new vortex has switched to the lower surface. (Lu and Dalton, 1966)

Figure 21: Wake vortex structure over several oscillations for $f_{ex}D/U=0.109$, $f_{ex}/f_w=1/2$ and A/D=0.237 (Rodriguez and Pruvost, 2000).
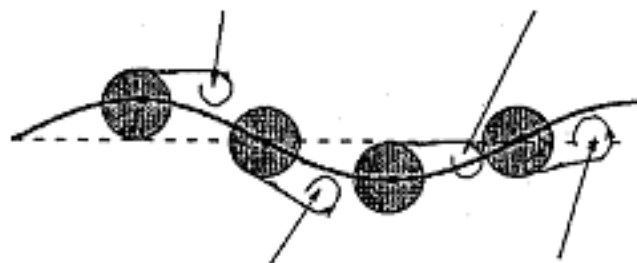
Presentation Notes: This figure shows both the in-line and transverse oscillations in a two degree-of-freedom oscillation. The influence of the reduced velocity (Vr) is quite clear. The lowest plot in the figure shows the trace of the oscillation that indicates quite clearly that the maximums of the in-line and transverse displacements do not occur simultaneously.

Figure 22:
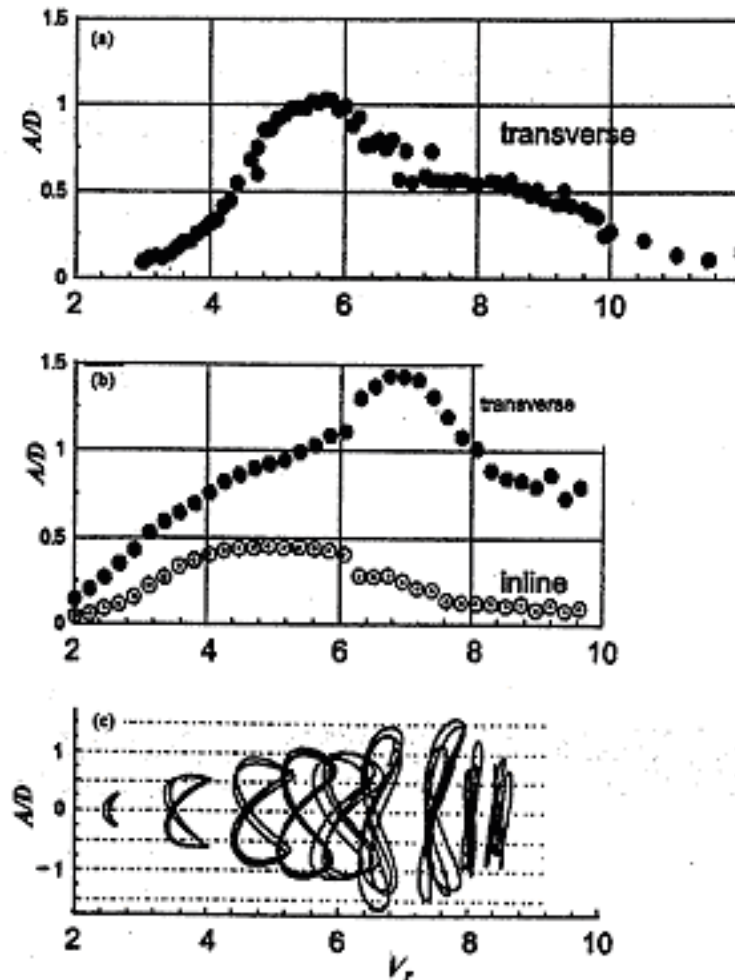
(a) One degree of freedom rigid cylinder (Re=30,000, L/D=26, m*=3.0, $\zeta=0.035$, m* $\zeta=0.105$). The amplitude A/D (1/10th highest average) reaches a maximum just a little over 1.0 at Vr $\cong 5.6$. There is no upper branch, but only a smooth increase in A/D; (b) a flexible cylinder (a pinned beam with 2-DOF) exhibits essentially the same overall behavior. However, the position of the maximum A/D is shifted to larger Vr (about 7) to larger A/D (about 1.5); (c) the maximums of the in-line and transverse motion trajectories do not occur simultaneously, the former precedes the latter, see also the forces in 22 (b). (from Triantafyllou, Techet, Hover, and Yue, 2003).

26

Presentation Notes: This figure contrasts the drag coefficient (C_d) vs. Reynolds Number (Re) and reduced velocity (Vr) for the stationary cylinder and the cylinder in VIV. The effect of shear in the approach flow is also present. Note that the C_d peak decreases as the shear increases.

Figure 23:
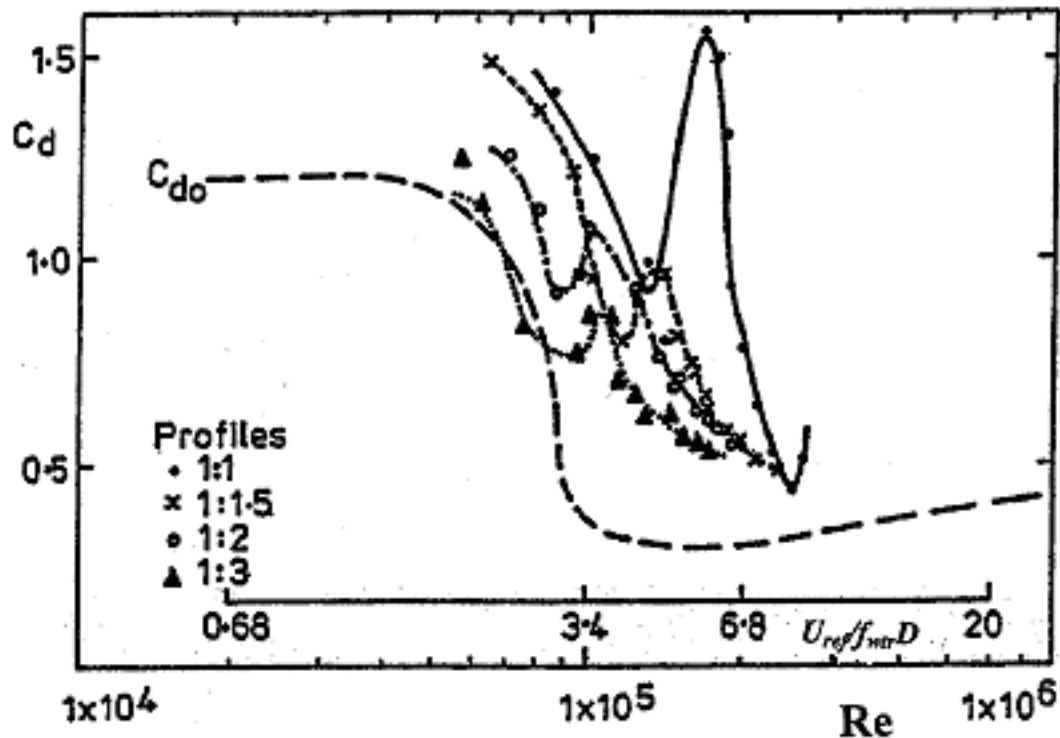
(a) The nature of the variation of C_d is like that of a smooth cylinder entering the critical transition, with C_d dropping sharply. The VIV (with 2-DOF) first arrests the drop in C_d and then increases it sharply, proving that VIV occurred within the zone of critical transition. The drag for the uniform flow ($U_{max}/U_{min}=1:1$) is dramatically amplified with respect to the rigid cylinder (at rest). As to the effects of shear, the maximums of C_d decrease with increasing shear and occur at smaller $U_{ref}/f_{wtr}D$ (Humphries and Walker, 1988).

Presentation Notes: This figure shows the A/D variation for different values of reduced velocity and different values of shear. Note that the A/D peak decreases as the shear increases.
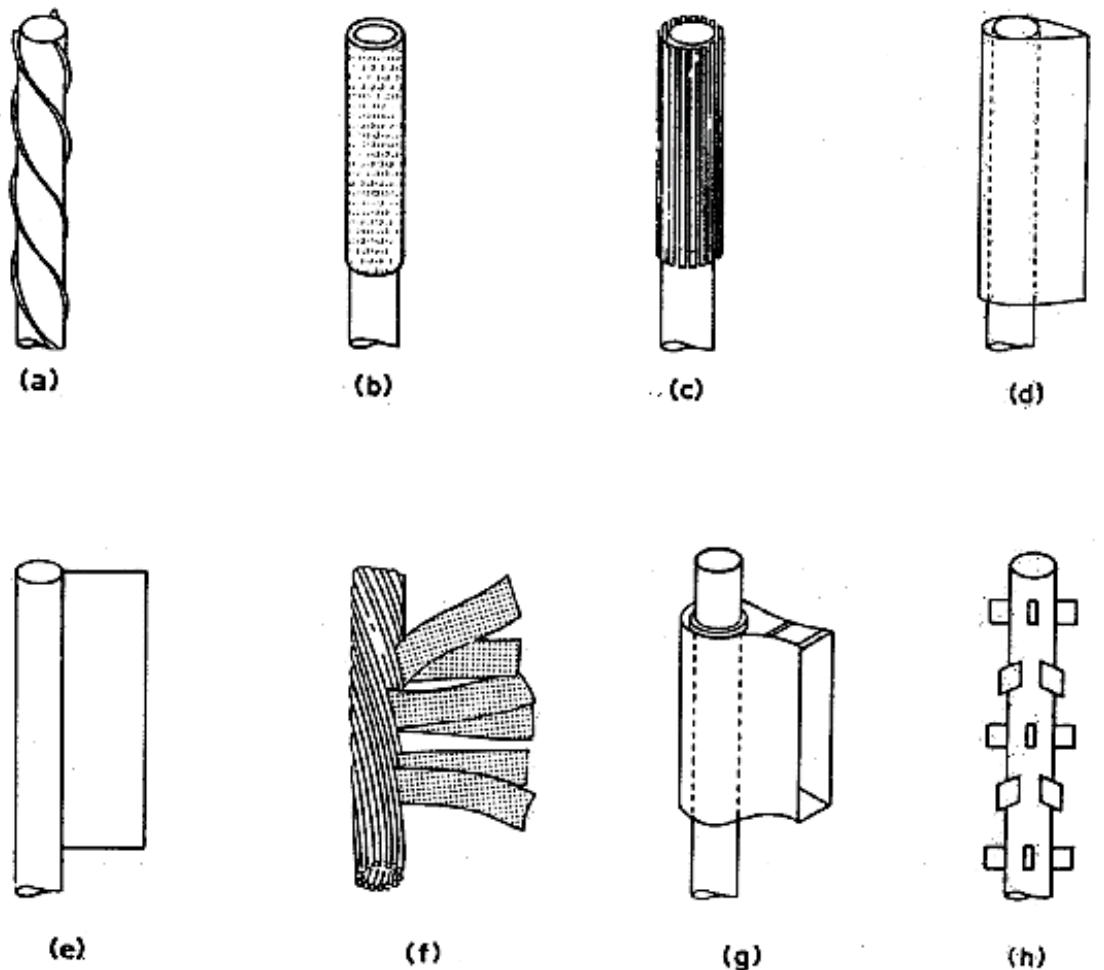
Figure 24:
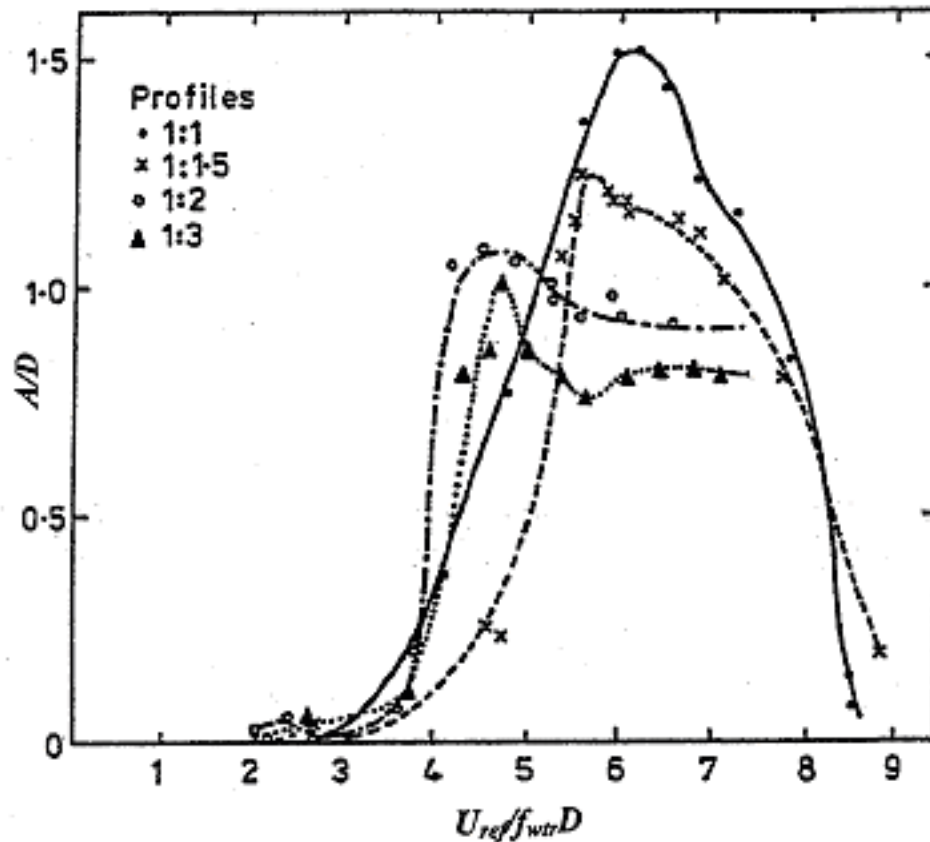
The maximum A/D for the no-shear case (about 1.5 a $V_{ref}/V_{wtr}D\cong6.2$) corresponds quite well with the in Fig. 22 (about 1.5 at $U_{ref}/f_{wtr}D\cong7$). With shear, the maximums of A/D occur with reduced peaks at smaller $U_{ref}/f_{wtr}D$ and decrease towards unity. It appears that shear extends the range of lock-in region. Even in the critical Re region, the occurrence of maximum C_d (at about $U_{ref}/f_{wtr}D\cong5.6$) precedes the occurrence of maximum A/D (at $U_{ref}/f_{wtr}D\cong6.2$), as in figures 22 (a) and (b) for the sub-critical flow (Humphries and Walker, 1988).

Presentation Notes: This figure shows eight of various devices used to influence vortex shedding and, thus, decrease VIV. The one most commonly used, for a flow which has the capability of changing directions, is depicted in (a). This configuration is called a spiral strake and it decreases considerably the longitudinal coherence of wake vortices that, in turn, diminishes VIV. Recently, a very promising version of (d) has been developed. This configuration is called a short fairing and the recent innovation is a mechanism that allows the chord length of the fairing to align itself with a possible change in the direction of the flow. This shape has the capability of decreasing drag as well as eliminating VIV. This short fairing is presently in limited use and seems to be working quite well.

Figure 25: Add-on devices for suppression of vortex-induced vibration of cylinders

(a) helical strake; (b) shroud; (c) axial slats; (d) streamlined fairing; (e) splitter; (f) ribboned cable; (g) pivoted guiding vane; (h) spoiler plates.
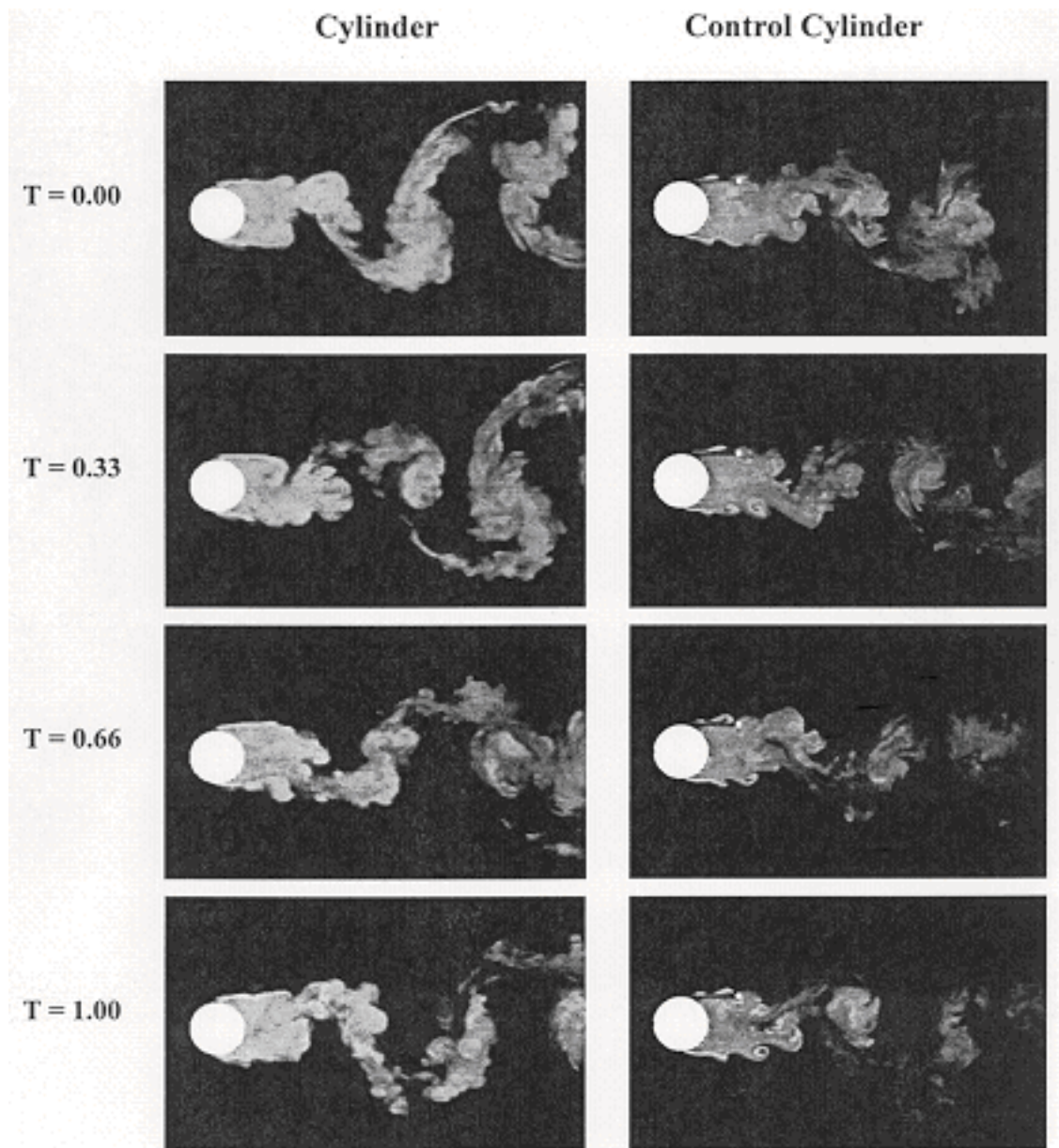
Presentation Notes: This figure is a flow visualization picture (at Re = 100) of flow past a bare fixed cylinder and flow past a fixed (primary) cylinder with a small diameter control cylinder in the shear layer on the upper side of the near wake. The presence of the control cylinder stabilizes the near wake and causes the near wake to be essentially time-independent. The result is a decrease in drag and a virtual elimination of the fluctuating lift. This configuration has two difficulties. The first is that the flow must be unidirectional and the second is that the control cylinder location depends on the Reynolds number.

Figure 26: Flow visualization comparison at Re=100, *x*=30, and R D=1.4
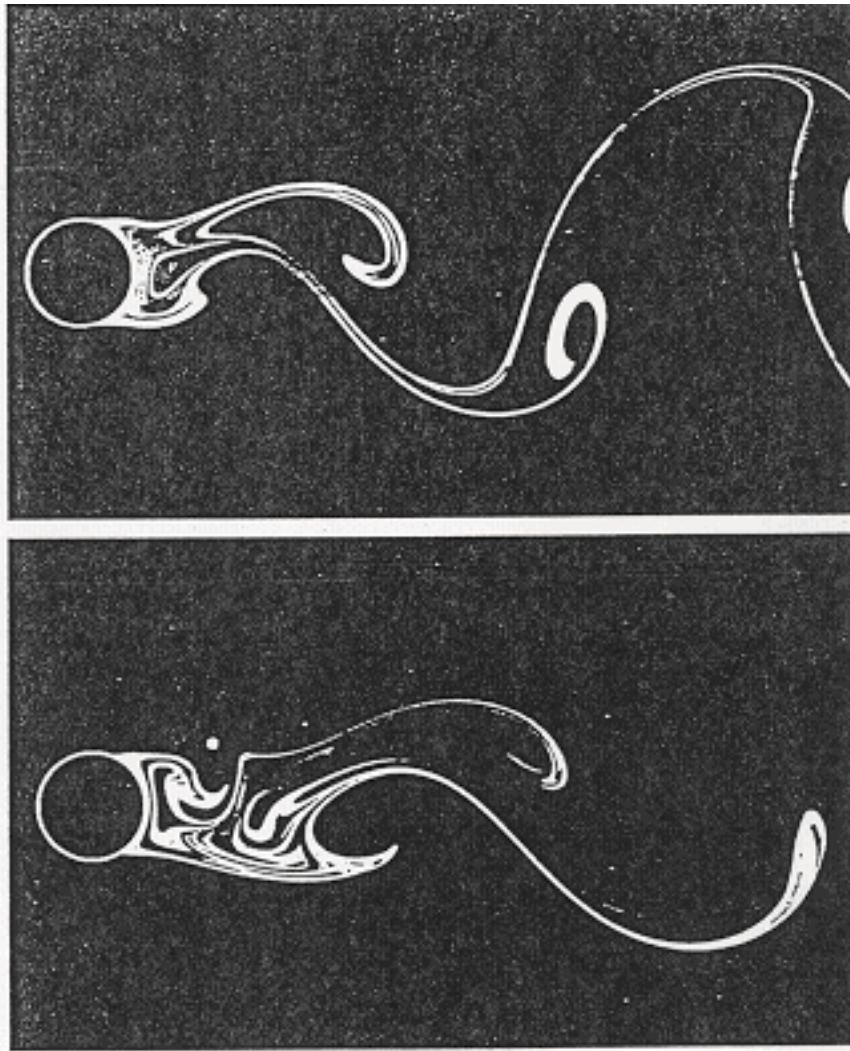
Presentation Notes: This figure shows essentially the same thing as shown in Figure 29 except that Re = 3000 in this figure. The near wake for the control-cylinder case is smaller and the time dependence in the wake vortices is suppressed until these vortices are further downstream. The result of the control-cylinder inclusion again is that the drag is decreased and the lift is essentially eliminated. The location of the control cylinder for this higher Reynolds number case is slightly different, making the application Re-dependent.

Figure 27:

Reynolds number =3000